UDC (549.057 + 549.5) : 544.77

O.M. Lavrynenko, Yu.S. Shchukin

F.D. Ovcharenko Institute of Bio-Colloid Chemistry of NAS of Ukraine
42, Acad. Vernadsky Ave., Kyiv-142, Ukraine, 03680
E-mail: alena-lavry@yandex.ru

DEVELOPMENT OF THE HYDROXYSULFATE GREEN RUST ON THE STEEL SURFACE CONTACTING WITH WATER FERRIC AND FERROUS SALT SOLUTIONS

Hydroxysulfate Green Rust $GR(SO_4^{2-})$ or sulfate fougerite is the typical member of the layered double hydroxide (LDH) family and plays an important role in the global biogeochemical cycle of iron and concomitant elements. The sulfate-bearing Green Rust is developed in the following environmental systems: mid-ocean ridge hydrothermal vents, volcanic systems, marine sedimentsand hydromorphic soils. Usually its formation in the nature is realized in seawater under corrosion processes. Due to high reductive properties and chemical activity of natural Green Rusts their study is highly complicated; consequently Green Rust formed under laboratory conditions is often used for modeling natural processes of mineral formation. The surface of iron alloys may be one of the suitable systems for the research of Green Rust development. So, we studied the development and phase transformation of the hydroxysulfate Green Rust on the surface of the steel 3 contacting with ferric and ferrous sulfate water solutions under oxidative and reductive conditions. The concentration of dissolved ferric and ferrous iron was chosen as 10, 100 and 1000 mg/dm³. The pH values were set at 3.5 and 6.5. The X-ray diffraction *in situ* was used as the main method of the research. The measurement was taken by the computer-aided equipment (DRON 3) supplied with two Seller slits and filtered emission of cobalt anode. The critical Woolf-Bragg angle was determined at around 80 °C. The XRD study permitted to see the processes of the development of the nanosized iron-oxygen minerals on the steel surface within 72—90 h. Scanning electron microscopy using JOEL-6700 microscope equipped by energy-dispersive and cathode-luminescence attachment was chosen as a visualization technique for description of the particle morphology. The structures of hydroxysulfate Green Rust, lepidocrocite and goethite belong to the main mineral phases formed on the steel surface under the RCD conditions. Magnetite particles appear on the steel surface when it contacts with low concentration of ferrous iron solutions in the wide range of pH. The simultaneous presence of schwertmannite, ferrihydrite and Fe(III)−Green Rust that are the components of the phase transformation chains points to the continuity of the phase formation process. The heterogeneity of the steel surface and presence of anodal and cathodal areas together with structural defects are found as other reason for the variety of mineral composition. The following chains of phase the transformation on the steel surface contacting with ferric and ferrous water solution are supposed: 1) schwertmannite → ferrihydrite) or goethite → Green Rust via dissolution-precipitation process in the corrosion pittings (anodal areas); 2) Green Rust → Fe(III)−GR and/or lepidocrocite via solid state transformation (catodal areas); 3) dissolved Green Rust or ferric and ferrous micellar species → magnetite under reductive conditions; 4) magnetite → lepidocrocite or goethite under oxidative conditions; 5) Green Rust → lepidocrocite in acid medium and 6) ferric and ferrous micellar species → nanomagnetite in alkaline medium.*

Keywords: Fe(II)−Fe(III) layered double hydroxides, hydroxysulfate Green Rust, nanoparticles, sulfate fougerite, schwertmannite, Fe(III)−Green Rust, lepidocrocite, magnetite, steel surface, *red-ox* conditions.

Introduction. Hydroxysulfate Green Rust II $GR(SO_4^{2-})$ or sulfate fougerite, that ideal formula is $Fe^{II}_4Fe^{III}_2(OH)_{12}SO_4^{2-} \cdot {\sim}8\,H_2O$, belongs to the layered double hydroxide family and plays an important role in the global biogeochemical cycle of iron and concomitant elements among the wide range of disperse iron-(oxy)hydroxide minerals, such as ferrihydrite, fougerite, schwertmannite, goethite, lepidocrocite etc. [15]. The formation of typical Green Rust structures is realized via interaction of ferric and ferrous species in natural waters

---

* Редколегія усвідомлює, що тема даної статті не відповідає тематиці "Мінералогічного журналу", однак отримані авторами результати можуть бути цікавими для мінералогів.

accompanied by a microbial activity and biomineralization process [19]. The appearance of abiogenically Green Rust is usually noticed when acidic iron-rich solutions are neutralized by country rock species [11] as well as when iron-reach rocks and minerals are weathering [8]. The most significant environmental systems, where the sulfate-bearing Green Rust mineral particles are present, can be the following: mid-ocean ridge hydrothermal vents [21, 38], volcanic systems [23], marine sediments [13], groundwaters [19] and hydromorphic soils [9, 20]. Usually hydroxysulfate Green Rust formation in the nature takes places in seawater under corrosion processes [36].

The analysis of the natural Green Rust samples is difficult because of its high reductive properties and chemical activity. Consequently the Green Rust formed under laboratory conditions is often used for modeling natural processes of mineral formation [18]. The obtaining of the Green Rust particle in a microbiological way is useful for the modeling of different biogeochemical processes and cycles [9, 17]. Whereas the chemical formation of hydroxysulfate Green Rust $GR(SO_4^{2-})$ under laboratory conditions is carried out via aerial oxidation of a ferrous hydroxide suspension in the presence of a slight excess of dissolved Fe^{2+} [16] or via ferric and ferrous basic salts or hydroxides co-precipitation [40]. The other way for the $GR(SO_4^{2-})$ preparation is its electrochemical deposition on the inert electrodes made of precious metals contacting with ferrous salt solution [6, 34] or its formation on the iron/steel surface in the presence of sulfate anions [25, 36]. The suitable system for the study of the Green Rust particle formation and transformation can be an iron alloy surface [29, 43].

The purpose of our work is to follow *in situ* the development and phase transformation of hydroxysulfate Green Rust II on the steel surface contacting with ferric and ferrous sulfate water solutions under oxidative and reductive conditions.

Objects and methods of the research. The formation of the hydroxysulfate Green Rust layer under the rotation corrosion dispergation (RCD) conditions was realized on the surface of the rotating disk electrode that alternately contacted with air oxygen and water dispersion medium. The electrode was made of the finished steel (St3). The experiment was carried out in a glove box to regulate the air access into the system. The main principle of the RCD method and the phase formation technique were described in details in our previous work [27, 29].

We selected ferric and ferrous sulfate salt solutions as the dispersion medium. The concentrations of dissolved ferric and ferrous iron 10, 100 and 1000 mg/dm³ were chosen. The pH values 3.5 and 6.5 were set.

We determined the mineral composition of the disperse phases applying X-ray diffraction (XRD) method. The measurement was taken by the computer-aided equipment (DRON 3) supplied with two Seller slits and filtered emission of cobalt anode $CoK\alpha$ in discrete conditions of plotting, with pitch of 0.1 degree and time of piling in every point 4 sec. X-ray emission was detected with help of the BDS-6 scintillation unit. The critical Woolf-Bragg angle was determined at around 80 °C. The additional module [26] was used for recording the development of mineral phases with the time on the steel surface (*in situ*). The mineral particles were identified according to the database of *ASTM Powder Diffraction File/International Centre for Diffraction Data. — Swartmore, Pensilvania, U.S.A. — 1977* and *JCPDS International Center for Diffraction Data* (1998) saved in the computer program PCPDFWIN v. 2.0. The XRD study permitted to see the processes of the development of the nanosized iron-oxygen minerals on the steel surface within 72—90 h. The crystal lattice parameters of mineral phases and the primary particle size (coherent scattering region, CSR), were calculated using the XRD-data [1]. Scanning electron microscopy (SEM) using JOEL-6700 microscope equipped by energy-dispersive and cathode-luminescence attachment was chosen as a visualization technique for description of the particle morphology.

Results and discussion. *The development of the hydroxysulfate Green Rust on the steel surface in the presence of the dissolved ferrous iron.* The study of the surface structure formation was carried out applying XRD method *in situ*. The iron-oxygen mineral phases were formed under free access of the air to the steel surface as well as under limited oxidation of the system. The concentration of the dissolved ferrous iron in the dispersion medium was 1000 mg/dm³, pH value was 6.5.

According to XRD-data (Fig. 1, *a*), *under oxidative conditions* the reflexes of the hydroxysulfate Green Rust $GR(SO_4^{2-})$ appear after 2 h of the steel

Fig. 1. XRD-pattern obtained under *in situ* condition when the steel surface was contacted with: *a* —FeSO₄ solution ($C_{Fe(II)}$ = 1000 mg/dm³, pH 6.5); *b* — Fe₂(SO₄)₃ solution ($C_{Fe(III)}$ = 1000 mg/dm³, pH 6.5). The numbers correspond to the mineral phases: *1* — Green Rust, *2* — goethite, *3* — ferrihydrite, *4* — iron, *5* — lepidocrocite

24

ISSN 0204-3548. Mineral. Journ. (Ukraine). 2015. 37, No 2
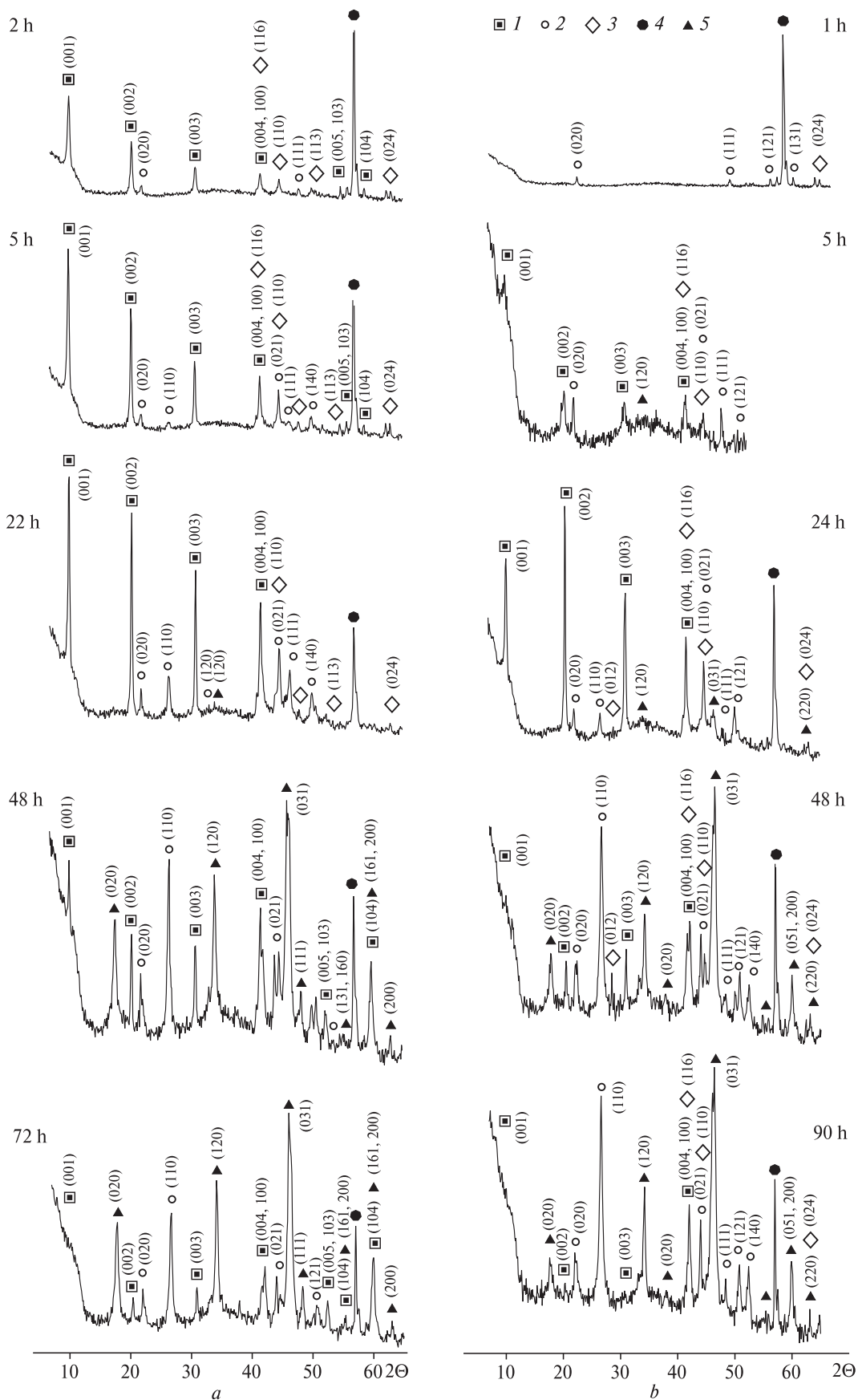
surface contact with $FeSO_4$ solution and then they are growing during next 20 h. The $GR(SO_4^{2-})$ reflexes (001), (002), (003), (004, 100), (005, 103) and (104) are clearly seen on the XRD pattern. At the same time some reflexes of ferrihydrite, goethite (111), hematite (116), (110), (113) and (024) are found on the pattern. The intensity of the Green Rust and goethite reflexes are growing during 24 h, but their relative quantities change: the $GR(SO_4^{2-})$ part is decreased whereas the α-FeOOH part is increased. The beginning of the increase of Green Rust peak intensity correlates with the appearance and increase of lepidocrocite reflexes: (120) at first and then (020), (031), (111), (131), (160), (161, 200) and (220). Such tendency is kept during 48 h up to the stationary state of the system. The disappearance of the hematite reflexes together with the small angle Green Rust reflexes suggests inclusion of α-Fe_2O_3 into crystal lattice of $GR(SO_4^{2-})$ as a structural unit. It is indicative that no magnetite/spinel ferrite reflexes are found even after 72 h of the contact of the steel surface with the dispersion medium.

The detailed analysis of the XRD patterns of Green Rust II permits to trace the development of the alteration of $GR(SO_4^{2-})$ crystal lattice. So, the reflexes of $GR(SO_4^{2-})$ formed within 5 h can be correlated with iron sulfate hydroxide with general composition $Fe_2(OH, SO_4)_{4.88}$ (JCPDS file 41-0014). The following lattice change leads to the displace-

ment of the interplanar distance (d_{001}) from 1.12 to 1.09 nm. Such structure was fixed from 22 to 48 h. The last form of the oxidized Green Rust II was registered after 72 h when the interplanar distance (d_{001}) shifted to 0.74 nm and the phase composition became $Fe_{3.6}Fe_{0.9}(O, OH, SO_4)_9$ called iron oxide sulfate hydroxide according to (JCPDS file no 13-0090). The presence of all characteristic peaks on the XRD patterns and compossibility of their relative intensities give us the grounds to identify the obtained mineral phases with the above mentioned forms of Green Rust II. An insignificant shift of all XRD-peaks to bigger angles takes place during "ageing" of the Green Rust II structure due to smaller cation radius of ferric iron in comparison with ferrous one. All forms of hydroxysulfate Green Rust belong to a hexagonal system.

The crystal lattice parameters and the average CSR area calculated for the surface structures are present in the summarizing Table 1. The particle size of the goethite gradually decreases from ~38 to ~11 nm probably because of the dissolution process that takes place in the system. On the contrary the oxidizing of the Green Rust and the rearrangement of its structure lead to increasing of the LDH particle size.

When the oxidation process is limited the first $GR(SO_4^{2-})$ reflexes (001), (002), (003), (004, 100) are identified during 1 h of the contact of the steel surface with the ferrous sulfate solution. At the same time the single magnetite reflex (311) is seen on the XRD-pattern. Such phase composition remains unchanged during 24 h. The single peak of goethite (110) points to the start of oxidation process. The iron oxyhydroxides (α-FeOOH and γ-FeOOH) with the admixture of Fe_3O_4 and $GR(SO_4^{2-})$ develop after 72 h of the phase formation process. The increase of the oxyhydroxide peak intensity correlates with the decrease of the LDH reflexes. The further development of the LDH surface structures is the same as under oxidizing conditions and it leads to the phase transformation of $GR(SO_4^{2-})$ into oxyhydroxides (α-FeOOH and γ-FeOOH). The weak magnetite reflexes (220), (311) and 400 as well as small angle Green Rust reflexes are seen on the XRD pattern. The amount of the magnetite peaks gradually increases during 72 h. XRD analysis of the sediments obtained from the steel surface and mineral phases of the near-surface film clearly shows the following: whereas the Green Rust and magnetite phases are associated with the surface layer, the goethite particles develop in the near surface layer.

Table 1. **The crystal lattice parameters and primary particle size of hydroxysulfate Green Rust formed on the steel surface when it was contacting with $FeSO_4$ and $Fe_2(SO_4)_3$ water solutions**

Cation concentration, mg/dm³	pH value	The cation	Time, h	$GR(SO_4^{2-})$		
				a	c	d
				nm		
10	3.5	Fe^{2+}	2	0.31551	1.10246	14.52
			5	0.31522	1.09423	17.30
			24	0.31391	1.09377	25.42
			72	—*	—	—
1000	6.5	Fe^{2+}	2	0.06715	0.01651	15.63
			4	0.06712	0.01651	17.05
			22	0.06804	0.01685	17.05
			48	0.06713	0.01656	20.84
			70	0.06713	0.01657	26.80
		Fe^{3+}	5	0.31605	1.10667	11.29
			24	0.31531	1.101741	20.33
			48	0.31532	1.09546	16.94
			90	—	—	—

N o t e. * — the mineral phase was not found.

26

ISSN 0204-3548. Mineral. Journ. (Ukraine). 2015. 37, No 2

The appearance of the GR(SO$_4^{2-}$) reflexes (001), (002), (003), (004, 100) under lower ferrous iron concentration 10 mg/dm^3, pH 3.5 and oxidative conditions is observed after 2 h of the process (Fig. 2, *a*). Their intensity grows during 5 h and then it gradually decreases and disappears. The magnetite reflexes (311), (400), (440) are shown after 2 h and the lepidocrocite reflexes (120), (031), (111), (200), (220) appear after 5 h. The intensity of both phases gradually increases until the system transfers into the stationary state (72 h).

The development of the hydroxysulfate Green Rust on the steel surface in the presence of the dissolved ferric iron. Probably, when the phase formation process on the steel surface takes place in the presence of a ferric salt solution, the *red-ox* conditions in the system become less important. So, the next experiment was carried out under oxidative and reductive conditions when the Fe$_2$(SO$_4$)$_3$ water solution ($C_{Fe(III)}$ = 1000 mg/dm^3, pH 6.5) was used as the dispersion medium. In both cases the following particles developed on the steel surface: GR(SO$_4^{2-}$), γ-FeOOH and α-FeOOH. The distinction lay only in the quantitative ratio of the components in the mineral mixtures as well as in the Green Rust disappearance during 24 h under reductive conditions. Fig. 1, *b* shows the XRD pattern obtained *in situ* under free access of air oxygen into the reaction area. The (001), (002), (003), (004, 100) GR(SO$_4^{2-}$) reflexes and (116), (110), (024) α-FeOOH reflexes were identified after 5 h of the process. The intensity of the Green Rust peaks gradually increased during 24 h and then it gradually decreased to the total disappearance during 90 h. Simultaneously, the (021), (111) peaks of goethite were identified after 5 h, but the first (120), (031), (220) lepidocrocite peaks were seen only after 24 h. Whereas the hematite peaks appeared on the XRD pattern after 5 h and remained there during 90 h as an additional phase. Perhaps, hematite got included into the crystal lattice of the ferrihydrite that could be an intermediate product of the Green Rust oxidation. The increase of the reflex intensity lasted until the system transferred into the stationary state. Whereas, the X-ray reflexes of the spinel ferrite (magnetite) did not appear even after 90 h of the phase formation process. Probably, Green Rust particles transformed into lepidocrocite and then goethite, as it was found in the previous case.

The (001), (002), (003), (004, 100) GR(SO$_4^{2-}$) reflexes are seen on the pattern after 6 h of the phase formation under reductive conditions and

then they disappear within 24 h. Simultaneously the isolated reflexes of magnetite (311), lepidocrocite (020) and goethite (110), (131) are present on the XRD pattern. Disappearance of the GR(SO$_4^{2-}$) can be explained by its phase transformation into iron oxyhydroxides, their relative quantity gradually grows during 72 h.

The Green Rust reflexes do not appear on the pattern when ferric iron (10 mg/dm^3) is added in the dispersion medium at pH value 3.5 (Fig. 2, *b*). But the (111), (220), (311), (400), (440) reflexes of magnetite are seen after 2 h and the (020), (120), (031), (111), (051, 200) lepidocrocite reflexes appear during 24 h. The increase of the lepidocrocite reflexes is more intensive in comparison with magnetite reflexes. Probably, Green Rust is not collected on the steel surface and it quickly transforms into lepidocrocite. At the same time, magnetite particles can be oxidized to lepidocrocite under the oxidative conditions. Such supposition confirms the decrease of magnetite reflexes after 24 h and the increase of a lepidocrocite part in the phase composition of the surface structures. The Green Rust peak (003) shifts from 11.066 to 11.016 nm within 24 h. In a similar way, the structure of GR(SO$_4^{2-}$) corresponds to the formula Fe$_2$(OH, SO$_4$)$_{4.88}$ (JCPDS No 41-0014). The crystal lattice parameters of mineral phases and the primary particle size, calculated according to XRD-data, are presented in Table 1. The obtained results clearly point out that the iron-oxygen structures formed under rotation-corrosion dispergation conditions belong to nanosized objects.

The relative quantity of the surface mineral phases formed on the steel surface was calculated using the X-ray diffraction data. We chose the most intensive picks for every mineral phase as maximum (1.0) and calculated the relative quantity of other smaller picks for the same phases. Whereas the total mass distribution of the mineral phases in the samples using semiquantitative X-ray diffraction method will be corrected only after XRD-equipment calibration. As it is shown in Table 2, the optimal conditions for the hydroxysulfate Green Rust formation were observed when the steel surface was contacting with ferrous sulfate solution ($C_{Fe(II)}$ = 1000 mg/dm^3 and pH 6.5) during 2—22 h. Lepidocrocite was mainly formed when the concentration of ferrous iron and pH value was lower ($C_{Fe(II)}$ = 1000 mg/dm^3 and pH 3.5). On the contrary, goethite as a dominant phase was formed in the presence of ferric sulfate solution when the ferric iron concentration was high ($C_{Fe(III)}$ = 1000 mg/

28

ISSN 0204-3548. Mineral. Journ. (Ukraine). 2015. 37, No 2
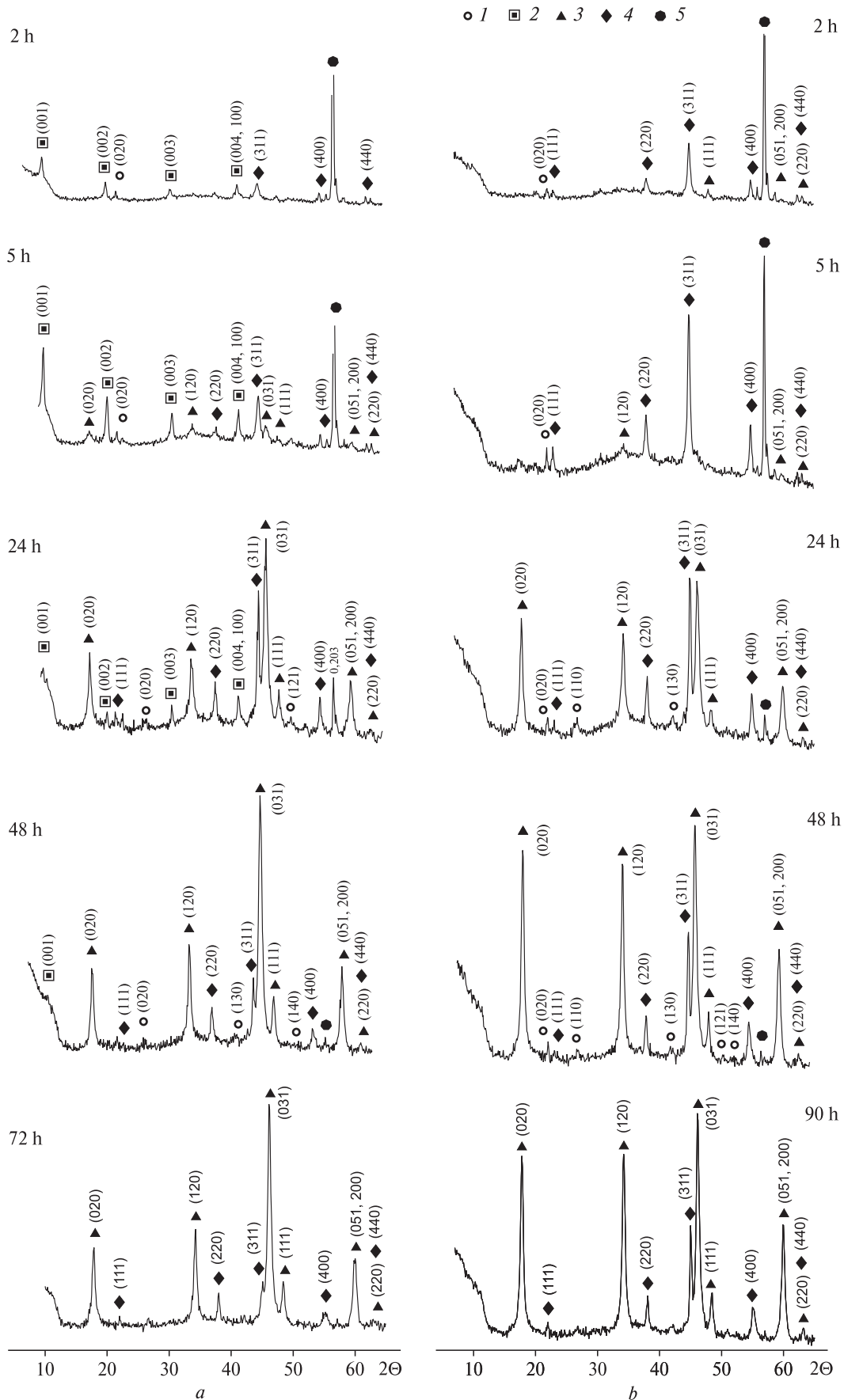
dm^3 and pH 6.5). The relative quantity of both iron (ferric) oxyhydroxides gradually increased and reached its maximum after 24 h of the process duration.

The morphology and chemical composition of the mineral phases formed on the steel surface contacting with ferrous and ferric sulfate water solutions. The study of the chemical composition of the Green Rust formed under RCD conditions when the steel surface was contacting with ferrous and ferric sulfate solutions (C_{Fe} = 1000 mg/dm^3, pH 6.5, T = = 20 °C) was carried out with the help of the scanning electron microscope JEOL-6700 fitted with EDS and cathode luminescence equipment. So, when GR(SO_4^{2-}) was formed in the presence of ferrous sulfate it is characterized by the following average values: Fe — 37.01—38.04; O — 55.98—56.49; S — 5.98—6.49 at. % or Fe — 65.02—66.14; O — 27.87—28.43; S — 5.97—6.55 wt. %. The structure of GR(SO_4^{2-}) formed in the presence of ferric sulfate includes Fe — 38.2; O — 55.9; S — 5.8; Si — 0.1 at. % or Fe — 66.27; O — 27.77; S — 5.82; Si — 0.14 wt. %. Thus, the Green Rust obtained in $Fe_2(SO_4)_3$ water solution is characterized by bigger amount of iron and smaller amount of sulfur and oxygen in comparison with the Green Rust formed in $FeSO_4$ water solution. The schwertmannite mineral appears as the second mineral phase when steel surface is contacting with ferric sulfate solution. Its chemical composition is: Fe — 37.11; O — 56.4; S — 6.4 at. % or Fe — 65.11; O — 28.3; S — 6.5 wt. %.

Usage of scanning electron microscopy permits to prove that the phase formation process on the steel surface is continuous. Simultaneously the primary iron oxygen particles co-exist with the products of their phase transformation and destruction. E. g. Fig. 3 shows the SEM images of the mineral phases formed on the steel surface contacting with $FeSO_4$ water solution ($C_{Fe(II)}$ = 100 mg/dm^3, pH 6.5, T = 20 °C); time of the contact 24—25 h.

The "hedge-hog" schwertmannite particles formed in corrosion pittings on the steel surface contacting with $FeSO_4$ water solution at $C_{Fe(II)}$ = = 1000 mg/dm^3 are present on the Fig. 3, *a*. Similar structures as well as schwertmannite "whisker" par-

ticles were recently discovered to contain the highly-disordered maghemite-like structural components present in ferrihydrite [31]. The oxidized Green Rust structure formed under such conditions is shown on Fig. 3, *b*. The next images show the iron-oxygen structures formed when the steel surface contacted with $Fe_2(SO_4)_3$ water solution ($C_{Fe(III)}$ = 100 mg/dm^3, pH value 6.5) under the RCD conditions. The "web-like" schwertmannite covered with iron oxyhydroxide plates are present on Fig 3, *c*. The structures that are shown on Fig. 3, *d* belong to ferrihydrite spherical particles. The particles on Fig. 3, *e* and 3, *f* may be related to the product of the solid-state Green Rust oxidizing — "ferric green rust" or Fe(III)—GR. The Fe(III)—GR obtained on the steel surface under oxidizing conditions is similar to Fe(III)—GR obtained in work [30]. Fig. 3, *f* corresponds to Fe(III)—GR covered with products of its dissolution-precipitation [5].

The colloid-chemical mechanisms of the hydroxysulfate Green Rust formation on the steel surface in the presence of dissolved ferric and ferrous species. The general reaction equation that describes the process of the hydroxysulfate Green Rust formation can be written as:

$$5\,Fe(OH)_2 + Fe^{2+} + SO_4^{2-} + 0.5\,O_2 +$$
$$+ 9\,H_2O \rightarrow Fe^{II}_4Fe^{III}_2(OH)_{12}SO_4 \cdot 8\,H_2O. \quad (1)$$
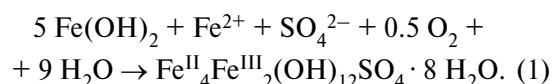
The SEM images confirmed that the Green Rust particle formation starts on the structural defects of

Table 2. **The relative quantity of the mineral phases formed on the steel surface when it contacted with ferric and ferrous sulfate water solutions**

Cations in the solution	Cation concentration, mg/dm^3	Time, h	Mineral		
			GR(SO_4^{2-})	γ-FeOOH	α-FeOOH
Fe^{2+}	10	2	0.25	—	—
		5	0.47	0.17	—
		24	0.05	0.64	0.09
		72	—*	**1.00**	0.11
Fe^{2+}	1000	2	0.70	—	—
		4	**1.00**	—	0.11
		22	0.76	—	0.46
		48	0.10	0.54	0.73
		70	—	0.74	0.76
Fe^{3+}		5	0.06	—	—
		24	0.53	—	0.20
		48	0.02	0.31	0.92
		90	—	0.22	**1.00**

N o t e. * — the mineral phase was not found.

Fig. 2. XRD-pattern obtained under *in situ* condition when the steel surface was contacted with: *a* — $FeSO_4$ solution ($C_{Fe(II)}$ = 10 mg/dm^3, pH 3.5), *b* — $Fe_2(SO_4)_3$ solution ($C_{Fe(III)}$ = 10 mg/dm^3, pH 3.5). The numbers correspond to the mineral phases: *1* — goethite, *2* — Green Rust, *3* — lepidocrocite, *4* — magnetite, *5* — iron
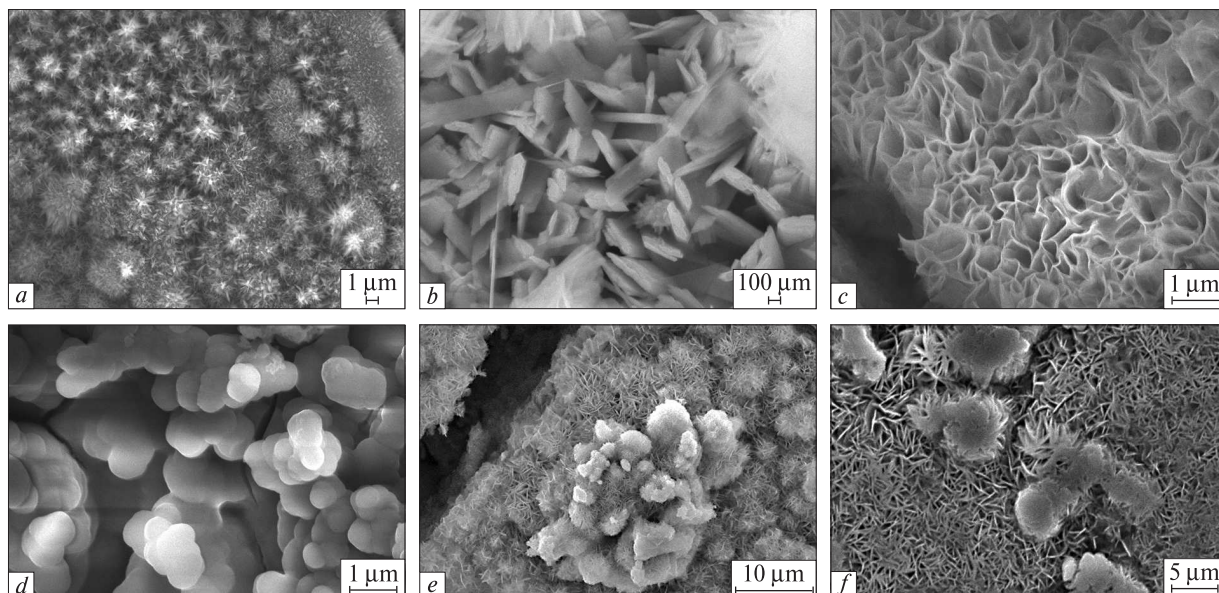
Fig. 3. The surface iron-oxygen disperse minerals formed under RCD condition when the steel electrode contacted with FeSO$_4$ water solution at $C_{Fe(II)}$ = 1000 mg/dm^3: *a* — "hedge-hog" of schwertmannite; *b* — the plates of Fe(III)−GR and goethite. The surface iron-oxygen disperse minerals formed under RCD condition when the steel electrode contacted with Fe$_2$(SO$_4$)$_3$ water solution at $C_{Fe(III)}$ = 100 mg/dm^3: *c* — "web-like" schwertmannite; *d* — ferrihydrite; *e* — Fe(III)−GR and the product of its dissolution; *f* — Fe(III)−GR

the steel surface and later it covers all surface area and forms the loose film. Due to the presence of ferrous iron in the lattice Green Rust its structure is unstable under oxidative condition and it may transform into the lepidocrocite phase during 2 h, as it was shown in our experimental part. Traditionally, three ways were found out for the oxidation of Green Rust into ferric oxyhydroxides: 1 — dissolution-precipitation process under slow oxidation condition leads to the obtaining of well-crystalline lepidocrocite and goethite; 2 — when the oxidizing process is faster than the dissolution the ferrihydrite particles appear in the system; 3 — when the oxidation is extremely fast or GR is dried before its oxidation in the air the Fe(III)−GR is formed on the iron surface [35]. It is indicative that the difference between the lepidocrocite formed by direct synthesis (precipitation) and the one obtained via Green Rust transformation due to galvanostatic oxidation can be explained by the particles orientation. In the first case the γ-FeOOH particles are preferentially oriented along (001), in the second case the lepidocrocite particles are randomly-oriented [7]. The randomly-oriented Green Rust and lepidocrocite particles can be seen on our SEM-images (Fig. 3, *g*, *h*, respectively). Co-precipitated lepidocrocite particles are shown on Fig. 3, *d*. Such result points to two independent processes of the lepidocrocite formation. Simultaneously the fol-lowing disperse minerals are present on the steel surface: ferrihydrite, goethite, schwertmannite, magnetite.

The study of the lepidocrocite particle development under corrosion conditions on the steel surface [41] permits to find the following oxidation stages accompanied by the phase transformation: 1 — ferrous species of Fe(OH)$_2$ → Fe(II)−Fe(III) LDH (Green Rust) layer; 2 — Green Rust → Fe(III)−Green Rust (ex-Green Rust); 3 — Fe(III)−Green Rust → γ-FeOOH and, probably, γ-FeOOH → α-FeOOH. Only lepidocrocite particles can be formed when the pH value is below 8.0. The mixture of Fe(III)−GR and γ-FeOOH appears in the pH range 8.0—8.9 and predominantly Fe(III)−GR exists in the system when pH higher than 8.9 [30]. The phase formation process on the steel surface under rotation-corrosion dispergation conditions is carried out in the pH range from 7.0 to 9.0 pH [2, 27]. Thus, both structures (lepidocrocite and Fe(III)−Green Rust) co-exist under RCD condition.

The average pH value of 7.0—9.0 in the reaction area does not permit to explain the appearance of the schwertmannite mineral. Schwertmannite is a ferric oxyhydroxysulfate with the general formula Fe$_8$O$_8$(OH)$_{8-2x}$(SO$_4$)$_x$ and $1 \leq x \leq 1.75$ [10]. The mineral is formed in the presence of high SO$_4^{2-}$ concentrations (from 1000 to 3000 mg/dm^3) [14]

30

ISSN 0204-3548. Mineral. Journ. (Ukraine). 2015. 37, No 2

at pH values between 2.5 and 4.5 [10, 45]. The explanation of its presence in our experiments can be found using electrochemical researches. Heterogeneity of the steel composition and the presence of anodal and cathodal areas on its surface create the differences in the local pH values that was confirmed using the complex indicator ferroxil (the mixture of phenol-phthalein and potassium ferricyanide) that had been added into electrolyte [3]. The anodal areas were colored to pink due to the hydroxyl liberation (alkali medium) and the cathodal areas were colored to blue due to the ferrous iron liberation (acid medium). Usually anodal areas associate with corrosion holes and pittings where not only pH value is low but also the concentration of sulfate and chloride anions is heightened. Such conditions are optimal for the schwertmannite precipitation. So, schwertmannite precipitates from supersaturated solutions mainly owing to the oxidation of ferrous iron to ferric iron and transforms with the time into goethite and jarosite [4, 8].

Probably schwertmannite hydrolyse resulting in the goethite (α-FeOOH) formation goes according to the following reaction [12]:

$$Fe_8O_8(OH)_{8-2x}(SO_4)_x + 2xH_2O \rightarrow$$
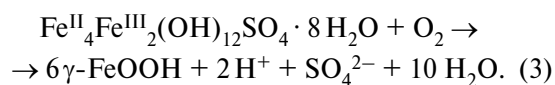$$\rightarrow 8\alpha\text{-FeOOH} + xSO_4^{2-} + 2xH^+. \quad (2)$$
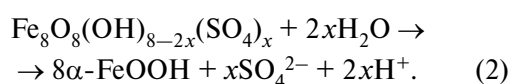
The phase transformation of schwertmannite into goethite in water solutions as well as in natural samples goes very slowly and depends on the pH value. E. g. the work [39] documented the increase of the transformation rates with increasing pH and fixed a complete transformation of schwertmannite to goethite in deionized water within ~100 days. The transformation time of >514 days was reported for natural samples incubated in original pore water [22]. But on the steel surface under the RCD conditions the presence of the schwertmannite "hedgehogs" was observed after 24 h. Probably the particle size can play an important role in the rate of the phase transformation. According to the study [5] the colloidal schwertmannite (~5 nm) that was formed at pH 2.8—4.5 under the hydrolysis of ferric species transformed within ~1 h into nanogoethite (<50 nm) at pH 5.5—6. The process catalyzed by Fe^{2+} decreases the stability of the schwertmannite crystals and leads to the structural rearrangements and formation of the more stable goethite particles. The solubility of ferrous iron decreases at pH > 7 and Fe^{2+} ions can be incorporated into the oxyhydroxide lattice with its further transformation into mixed Fe^{2+}/Fe^{3+} hydroxide sheets as primary

building units of Green Rust. At that sulfate ions as a part of schwertmannite crystal lattice adsorbed on the goethite surface and finally intercalated in the GR lattice. Thus study [5] showed that schwertmannite and nanogoethite are the only precursors for the formation of GR(SO_4^{2-}).

On the contrary the study [31] postulated the schwertmannite as an intermediate phase (in terms of crystallinity and kinetics of formation) to the least and most crystalline forms of two- and six-line ferrihydrite, respectively.

The analysis of the mass-balance and E_h — pH diagrams shows [37] that when both Fe^{2+} and SO_4^{2-} are present in the dispersion medium the magnetite particles are never observed as an intermediate product of Green Rust oxidation, only lepidocrocite can be formed in the system. The same result was shown in [44] where the lepidocrocite particles as well as the goethite particles were formed due to the process of the Green Rust oxidation. According to the diagram of electrochemical potential (E) — pH, only three mineral phases $Fe(OH)_2$, Green Rust and α-FeOOH) exist under the following condition: the range of pH values from 7.0 to 9.0 and the electrode potential area ranges from -0.45 to -0.25 V. Such physicochemical conditions are similar to the RCD condition in the iron based systems. The selective formation of either lepidocrocite or goethite particles strongly depend on the iron oxidation [24]. The elements added to weathering steels may accelerate transformation of γ-FeOOH to α-FeOOH [44]. The general reaction of the hydroxysulfate Green Rust oxidation into iron oxyhydroxide (lepidocrocite) under the RCD conditions may be the following:

$$Fe^{II}_4Fe^{III}_2(OH)_{12}SO_4 \cdot 8H_2O + O_2 \rightarrow$$
$$\rightarrow 6\gamma\text{-FeOOH} + 2H^+ + SO_4^{2-} + 10H_2O. \quad (3)$$

Green Rust as a precursor of magnetite was mentioned in some corrosion investigations [33]. On the contrary, according to [43] only the direct oxidation of the ferric and ferrous complexes $Fe(OH)_x^{(3-x)}$ and $Fe(OH)_y^{(2-y)}$ leads to the formation of the magnetite particles under corrosion conditions. The study of [32] confirms that the $GR_2(SO_4^{2-})$ can be converted into α-FeOOH and Fe_3O_4 particles through the dissolution and precipitation of ferrous and ferric compounds in the aqueous solution. But the research [42] demonstrates that the formation of magnetite due to dissolution-precipitation process can be realized under N_2 atmosphere (under anoxic conditions). The

similar reductive condition can be observed when the near surface layer is formed during the RCD process. According to our XRD data, the magnetite reflexes are present on the patterns obtained when the oxidation of the system is limited or the concentration of ferric and ferrous iron in the dispersion medium is small. The additional experiment shows that when the steel surface contacts with distilled water and is further substituted with the ferrous sulfate solution it does not lead to formation of magnetite particles [28]. Only $GR(SO_4^{2-})$ and iron oxyhydroxides are present on the steel surface. So, we state that the magnetite formation is realized via interaction of ferric and ferrous dissolved species but not via direct solid-state transformation of the Green Rust particles into magnetite.

Also, the analysis of our experimental data points to the few independent ways for the development of nanosized mineral phases on the steel surface contacting with ferric and ferrous water solutions under the RCD conditions. The heterogeneity of the steel surface, the presence of anodal and cathodal areas, surface defects and pittings lead to the creation of local physical-chemical conditions on the small parts of steel surface. In particular the heterogeneousness of the steel substrate for the particle formation can be denoted as a dominant cause of the iron-oxygen mineral variability. The formation of the primary particles changes the local physical-chemical conditions, especially pH value and oxygen quantity, that are the critical parameters for their further development. The chemical composition of dispersion medium makes additional alterations in the development of minerals. For example, the presence of the dissolved ferric iron (as a strong oxidant) leads to increasing of corrosion processes and reducing of ferric iron in cathodal areas [3]. Our results permit to trace the development of the following mineral phases: hydroxysulfate Green Rust, lepidocrocite, goethite and magnetite. The presence of other mineral phases on the steel surface can be fixed only on the SEM images. X-ray diffraction method does not show the reflexes of the two- and six-line ferrihydrite and schwertmannite because they can be overlapped by iron oxyhydroxide peaks as well as the quantity of such mineral phases is not enough (<5 %) for XRD-identification.

The most probable phase transformations on the steel surface contacting with ferric and ferrous water solution at pH 3.5—9.0 are the following: 1. The appearance of schwertmannite in pittings (anodal areas), its phase transformation into ferrihydrite or goethite and further into Green Rust via dissolution-precipitation; 2. The formation of Green Rust on cathodal areas via interaction of ferric and ferrous micellar species and its solid state transformation into Fe(III)−GR or lepidocrocite under oxidative conditions as well as its dissolution and precipitation into lepidocrocite and goethite; 3. The precipitation of magnetite via the interaction of the ferric and ferrous micellar species or via dissolution of Green Rust under reductive conditions; 4. The oxidation of magnetite followed by formation of lepidocrocite or goethite. The phase transformation process on the steel surface contacted with $FeSO_4$ water solution under acid conditions ($C_{Fe(II)} = 1000$ mg/dm^3, pH 1.5) can be described via Green Rust formation, probably as a result of schwertmannite dissolution, and its further solid state transformation into lepidocrocite. General process on the steel surface contacted with alkaline solution ($C_{Fe(II)} = 1000$ mg/dm^3, pH 11.5) in the presence of ferrous species connected with the formation of magnetite nanoparticles.

Conclusions. 1. The structures of hydroxysulfate Green Rust, lepidocrocite and goethite belong to the main mineral phases formed on the steel surface under oxidative and reductive conditions. Magnetite particles appear on the steel surface when it contacts with low concentration of ferrous iron solutions in the wide range of pH.

2. Schwertmannite, ferrihydrite and Fe(III)−Green Rust are clearly seen on the SEM images as intermediate phases. The simultaneous presence of different minerals that are the components of the phase transformation chains points to the continuity of the phase formation process. The heterogeneity of the steel surface and presence of anodal and cathodal areas together with structural defects are found as other reason for the variety of mineral composition.

3. The following chains of phases indicating transformation on the steel surface contacting with ferric and ferrous water solution are supposed: 1) schwertmannite → ferrihydrite) or goethite → Green Rust via dissolution-precipitation process in the corrosion pittings (anodal areas); 2) Green Rust → Fe(III)−GR and/or lepidocrocite via solid state transformation (cathodal areas); 3) dissolved Green Rust or ferric and ferrous micellar species → magnetite under reductive conditions; 4) magnetite → lepidocrocite or goethite under oxidative conditions; 5) Green Rust → lepidocrocite in acid medium and 6) ferric and ferrous micellar species → nanomagnetite in alkaline medium.

32

ISSN 0204-3548. Mineral. Journ. (Ukraine). 2015. 37, No 2

REFERENCES

1. *Гинье А.* Рентгенография кристаллов: пер с фр. — М. : Физматгиз, 1961. — 604 с.

2. *Лавриненко О.М.* Одержання композиційних структурованих систем на основі ферум-оксигенвмісних мінералів, їх структура та властивості: Автореф. дис. ... д-ра хім. наук. — К., 2013. — 40 с.

3. *Эванс Ю.Р.* Коррозия и окисление металлов (Теоретические основы и их практическое применение): пер. с англ. — М. : Машгиз, 1962. — 856 с.

4. *Acero P., Ayora C., Torrento C., Nieto J.-M.* The behaviour of trace elements during schwertmannite precipitation and subsequent transformation into goethite and jarosite // Geochim. et cosmochim. acta. — 2006. — **70**. — P. 4130—4139.

5. *Ahmed A. M., Benning L.G., Kakonyi G., Sumoondur A.D., Terrill N.J., Shaw S.* Formation of Green Rust Sulfate: A Combined in Situ Time-Resolved X-ray Scattering and Electrochemical Study // Langmuir. — 2010. — **26**, No 9. — P. 6593—6603.

6. *Antony H., Labri, A., Rouchaud J. C., Legranda L., Chausséa A.* Study of FeII /FeIII ratio in thin films of carbonate or sulphate green rusts obtained by potentiostatic electrosynthesis // Electrochim. acta. — 2008. — **53**. — P. 7173—7181.

7. *Antony H., Peulon S., Legrand L., Chausse A.* Electrochemical synthesis of lepidocrocite thin films on gold substrate — EQCM, IRRAS, SEM and XRD study // Electrochim. acta. — 2004. — **50**. — P. 1015—1021.

8. *Barham R.J.* Schwertmannite: A unique mineral, contains a replaceable ligand, transforms to jarosites, hematitesand / or basic iron sulphate // J. Mater. Res. — 1997. — **12**. — P. 2751—2758.

9. *Berthelin J., Ona-Nguema G., Stemmler S., Quantin C., Abdelmoula M., Jorand F.* Bioreduction of ferric species and biogenesis of green rusts in soils // C. r. Géosci. — 2006. — **338**, No 6—7. — P. 447—455. — Doi: 10.1016/j.crte.2006.04.013.

10. *Bigham J.M., Carlson L., Murad E.* Schwertmannite a new iron oxyhydrohysulfate from Pyha¨salmi, Finlandand other localities // Miner. Mag. — 1994. — **58**. — P. 641—648.

11. *Bigham J.M., Nordstrom D.K.* Iron and aluminum hydroxysulfates from acid sulfate water // Sulfate Minerals: Crystallography, Geochemistryand Environmental Significance / Ed. C.N. Alpers et al. — 2000. — P. 351—403. — (Revs in Mineralogy ; Vol. 40).

12. *Bigham J.M., Schwertmann U., Traina S.J., Winland R.L., Wolf M.* Schwertmannite and the chemical modelling of iron in acid sulphate waters // Geochim. et cosmochim. acta. — 1996. — **60**. — P. 2111—2121.

13. *Carey E., Taillefert M.* The role of soluble Fe(III) in the cycling of iron and sulfur in coastal marine sediments // Limnol. and Oceanogr. — 2005. — **50**. — P. 1129—1141.

14. *Carlson L.* Mineralogy of ochreous precipitates formed from mine effluents // Modern approaches to ore and environment mineralogy: Extended Abstract of Mini Sympos (Espoo Finland, 11—17 June 2000). — P. 3—4, available at: http://tupa.gtk.fi/julkaisu/opas/op_048.pdf.

15. *Chaves L.H.G.* The role of green rust in the environment: A review // Rev. bras. eng. agrHc. ambient. — 2005. — **9**, No 2. — P. 1—9. — Doi: 10.1590/S1415-43662005000200021.

16. *Detournay J., De Miranda L., Dérie R., Ghodsi M.* The region of stability of green rust II in the electrochemical potential — pH equilibrium diagram of iron sulphate medium // Corros. Sci. — 1975. — **15**, Is. 5. — P. 295—306.

17. *Dinh H.T., Kuever J., Mußmann M., Hassel A.W., Stratmann M., Widdel F.* Iron corrosion by novel anaerobic microorganisms // Nature. — 2004. — No 427. — P. 829—832. — Doi: 10.1038/nature02321.

18. *Feder F., Trolard F., Klingelhöfer G., Bourrié G.* In situ Mössbauer spectroscopy: Evidence for green rust (fougerite) in a gleysol and its mineralogical transformations with time and depth // Geochim. et cosmochim. acta. — 2005. — **69**, No 18. — P. 4463—4483.

19. *Fredrickson J.K., Zachara J.M., Kennedy D.W., Dong H., Onstott T.C., Hinman N.W., Li S.-M.* Biogenic iron mineralization accompanying the dissimilatory reduction of hydrous ferric oxide by a groundwater bacterium // Geochim. et cosmochim. acta. — 1998. — **62**, No 19—20. — P. 3239—3257.

20. *Génin J.-M.R., Bourrié G., Trolard F., Abdelmoula M., Jaffrezic A., Refait P., Maître V., Humbert B., Herbillon A.* Thermodynamic equilibria in aqueous suspensions of synthetic and natural Fe(II)—Fe(III) green rusts: Occurrences of the mineral in hydromorphic soils // Environ. Sci. and Technol. — 1998. — **32**. — P. 1058—1068.

21. *German C.R., von Damm K.L.* Hydrothermal processes // Treatise Geochem. — 2004. — **6**. — P. 181—222.

22. *Jonsson J., Persson P., Sjoberg S., Lovgren L.* Schwertmannite precipitated from acid mine drainage: phase transformation, sulphate release and surface properties // Appl. Geochem. — 2005. — **20**. — P. 179—191.

23. *Kennedy C.B., Scott S.D., Ferris F.G.* Ultra structure and potential sub-seafloor evidence of bacteriogenic iron oxides from axial volcano, Juande Fuca Ridge, north-east Pacific Ocean // FEMS Microbiol. Ecol. — 2002. — **1457**. — P. 1—8.

24. *Kimijima K., Kiyoshi K., Suzuki S., Muramatsu A.* Current Advances in materials and processes // ISIJ. — 2005. —**18**. — P. 1673.

25. *Lair V., Antony H., Legrand L., Chausse' A.* Electrochemical reduction of ferric corrosion products and evaluation of galvanic coupling with iron // Corros. Sci. — 2006. — **48**. — P. 2050—2063.
26. *Lavrynenko O.M., Korol Ya.D., Netreba S.V., Prokopenko V.A.* Kinetic regularity of the formation of Fe(II)—Fe(III) LDH structures (Green Rust) on the steel surface in presence of the $FeSO_4$ and $Fe_2(SO_4)_3$ water solutions // Chem., Phys. and Technol. Surf. — 2010. — **1**, No 3. — P. 338—342.
27. *Lavrynenko O.M., Kovalchuk V.I., Netreba S.V., Ulberg Z.R.* New rotation-corrosion dispergation method for obtaining of iron-oxygen nanoparticles // Nanostudies. — 2013. — **7**. — P. 295—322.
28. *Lavrynenko O.M., Shchukin Yu.S., Pavlenko O.Yu., Kosorukov P.A.* The features of the non-stoichiometric cobalt spinel ferrite and magnetite nanoparticle formation under rotation-corrosion dispergation conditions // Наноструктур. материаловедение. — 2014. — N 1. — P. 3—26.
29. *Lavrynenko O.M., Shchukin Yu.S.* Development of the hydroxycarbonate Green Rust on the steel surface contacting with water dispersion medium in the temperature range from 3 to 70 °C // Mineral. Journ. (Ukraine). — 2015. — **37**, No 1. — P. 22—33.
30. *Legrand L., Mazerolles L., Chausse A.* The oxidation of carbonate green rust into ferric phases: solid-state reaction or transformation via solution // Geochim. et cosmochim. acta. — 2004. — **68**, No 17. — P. 3497—3507.
31. *Loan M., Richmond W.R., Parkinson G.M.* On the crystal growth of nanoscale schwertmannite // J. Cryst. Growth. — 2005. — **275**. — P. 1875—1881.
32. *Olowe A.A., Génin J.-M. R., Bauer Ph.* Mössbauer effect evidence of a ferrous sulphate layer in the structure of green rust 2 and its atmospheric oxidation // Hyperfine Interact. — 1989. — **46**. — P. 437—443.
33. *Perales O., Umetsu Y.* ORP-monitored magnetite generation from aqueous solutions at low temperatures // Hydrometallurgy. — 2000. — **55**. — P. 35—56.
34. *Peulon S., Legrand L., Antony H., Chaussé A.* Electrochemical deposition of thin films of green rusts 1 and 2 on inert gold substrate // Electrochem. Commun. — 2003. — **5**. — P. 208—213.
35. *Refait Ph., Bernali O., Abdelmoula M., Genin J.-M.R.* Formation of ferric green rust and/or ferrihydrite by fast oxidation of iron (II—III) hydroxychloride green rust // Corros. Sci. — 2003. — **45**. — P. 2435—2449.
36. *Refait P., Memet, J.-B., Bon C., Sabota R., Génin J.-M.R.* Formation of the Fe(II)-Fe (III) hydroxysulphate green rust during marine corrosion of steel // Corros. Sci. — 2003. — **45**, No 4. — P. 833—845.
37. *Ruby C., Gehin A., Aissa R., Genin J.-M.R.* Mass-balance and Eh—pH diagrams of Fe^{II-III} green rust in aqueous sulphated solution // Corros. Sci. — 2006. — **48**. — P. 3824—3837.
38. *Russell M.J., Hall A.J., Boyce A.J., Fallick A.E.* On Hydrothermal Convection Systems and the Emergence of Life // Bull. Soc. Econ. Geol. — 2005. — **100**, No 3. — P. 419—438.
39. *Schwertmann U., Carlson L.* The pH-dependent transformation of schwertmannite to goethite at 25 °C // Clay Miner. — 2005. — **40**. — P. 63—66.
40. *Schwertmann U., Cornell R.M.* Iron oxides in the laboratory: preparation and haracterization. — Weinheim – New York – Bazel – Cambridge, 2000. — 188 p.
41. *Schwertmann U., Fechter H.* The formation of Green Rust and its transformation to lepidocrocite // Clay Miner. — 1994. — **29**. — P. 87—92.
42. *Tamaura Y., Yoshida T., Katsura T.* The synthesis of green rust II (Fe^{III}_1-Fe^{II}_2) and its spontaneous transformation into Fe_3O_4 // Bull. Chem. Soc. Jap. — 1984. — **57**. — P. 2411—2416.
43. *Washeda Y., Suzuki S.* Characterization of Corrosion products on Steel Surface. — Springer, 2005. — 297 p.
44. *Yu J.-Y., Heo B., Choi I.-K., Cho J.-P., Chang H.-W.* Apparent solubilities of schwertmannite and ferrihydrite in natural stream waters polluted by mine drainage // Geochim. et cosmochim. acta. — 1999. — **63**. — P. 3407—3416.
45. *Yu J.-Y., Park M., Kim J.* Solubilities of synthetic schwertmannite and ferrihydrite // Geochem. J. — 2002. — **36**, No 2. — P. 119—132.

1. Guignet, A. (1961), *Rentgenografija kristallov*, Fizmatgiz, Moskva, 604 p.
2. Lavrynenko, O.M. (2013), *Oderzhannya kompozitsiinikh strukturovanikh sistem na osnovi ferum-oksigenvmisnikh mineraliv, ikh struktura ta vlastivosti*, Avtoref. dys. d-ra himicheskih nauk, Kyiv, 40 p.
3. Evans, J.R. (1962), *Korrozija i okislenie metallov (Teoreticheskie osnovy i ih prakticheskoe primenenie)*, Mashgiz, Moskva, 856 p.
4. Acero, P., Ayora, C., Torrento, C. and Nieto, J.-M. (2006), *Geochim. et cosmochim. acta*, Vol. 70, pp. 4130-4139.
5. Ahmed, A.M., Benning, L.G., Kakonyi, G., Sumoondur, A.D., Terrill, N.J. and Shaw, S. (2010), *Langmuir*, Vol. 26 No 9, pp. 6593-6603.
6. Antony, H., Labrit, A., Rouchaud, J.C., Legranda, L. and Chauss a, A. (2008), *Electrochim. acta*, Vol. 53, pp. 7173-7181.
7. Antony, H., Peulon, S., Legrand, L. and Chausse, A. (2004), *Electrochim. acta*, Vol. 50, pp. 1015-1021.
8. Barham, R.J. (1997), *J. Mater. Res.*, Vol. 12, pp. 2751-2758.
9. Berthelin, J., Ona-Nguema, G., Stemmler, S., Quantin, C., Abdelmoula, M. and Jorand, F. (2006), *C. r. Géosci.*, Vol. 338 No 6-7, pp. 447-455.
10. Bigham, J.M., Carlson, L. and Murad, E. (1994), *Miner. Mag.*, Vol. 58, pp. 641-648.
11. Bigham, J.M. and Nordstrom, D.K. (2000), in Alpers, C.N. (ed.), *Sulfate Minerals: Crystallography, Geochemistryand Environmental Significance,* Vol. 40, pp. 351-403.

12. Bigham, J.M., Schwertmann, U., Traina, S.J., Winland, R.L. and Wolf, M. (1996), *Geochim. et cosmochim. acta*, Vol. 60, pp. 2111-2121.
13. Carey, E. and Taillefert, M. (2005), *Limnol. and Oceanogr.*, Vol. 50, pp. 1129-1141.
14. Carlson, L. (2000), *Modern approaches to ore and environment mineralogy*: *Extended Abstract of Mini Sympos*, (Espoo Finland, 11-17 June 2000), pp. 3-4, available at: http://tupa.gtk.fi/julkaisu/opas/op_048.pdf.
15. Chaves, L.H.G. (2005), Rev. bras. eng. agrHc. ambient., Vol. 9 No 2, pp. 1-9, doi: 10.1590/S1415-43662005000200021.
16. Detournay, J., De Miranda, L., Dérie, R. and Ghodsi, M. (1975), *Corros. Sci.,* Vol. 15 No 5, pp. 295-306.
17. Dinh, H.T., Kuever, J., Mußmann, M., Hassel, A.W., Stratmann, M. and Widdel, F. (2004), *Nature*, No 427, pp. 829-832.
18. Feder, F., Trolard, F., Klingelhöferand, G. and Bourrié, G. (2005), *Geochim. et cosmochim. acta*, Vol. 69 No 18, pp. 4463-4483.
19. Fredrickson, J.K., Zachara, J.M., Kennedy, D.W., Dong, H., Onstott, T.C., Hinman, N.W. and Li, S.-M. (1998), *Geochim. et cosmochim. acta*, Vol. 62 No 19-20, pp. 3239-3257.
20. Génin, J.-M.R., Bourrié, G., Trolard, F., Abdelmoula, M., Jaffrezic, A., Refait, P., Maître, V., Humbert, B. and Herbillon, A. (1998), *Environ. Sci. and Technol.,* Vol. 32, pp. 1058-1068.
21. German, C.R. and von Damm, K.L. (2004), *Treatise Geochem.*, Vol. 6, pp. 181-222.
22. Jonsson, J., Persson, P., Sjoberg, S. and Lovgren, L. (2005), *Appl. Geochem.,* Vol. 20, pp. 179-191.
23. Kennedy, C.B., Scott, S.D. and Ferris, F.G. (2002), *FEMS Microbiol. Ecol.*, Vol. 1457, pp. 1-8.
24. Kimijima, K., Kiyoshi, K., Suzuki, S. and Muramatsu, A. (2005), *ISIJ*, Vol. 18, p. 1673.
25. Lair, V., Antony, H., Legrand, L. and Chausse´, A. (2006), *Corros. Sci.*, Vol. 48, pp. 2050-2063.
26. Lavrynenko, O.M., Korol, Ya.D., Netreba, S.V. and Prokopenko, V.A. (2010), *Chem., Phys. and Technol. Surf.*, Vol. 1 No 3, pp. 338-342.
27. Lavrynenko, O.M., Kovalchuk, V.I., Netreba, S.V. and Ulberg, Z.R. (2013), *Nanostudies*, No 7, pp. 295-322.
28. Lavrynenko, O.M., Shchukin, Yu.S., Pavlenko, O.Yu. and Kosorukov, P.A. (2014), *Nanostruktur. materialovedenie*, Kyiv, Ukraine, No 1, pp. 3-26.
29. Lavrynenko, O.M. and Shchukin, Yu.S. (2015), *Mineral. Journ. (Ukraine),* Kyiv, Ukraine, Vol. 37 No 1, pp. 22-33.
30. Legrand, L., Mazerolles, L. and Chausse, A. (2004), *Geochim. et cosmochim. acta*, Vol. 68 No 17, pp. 3497-3507.
31. Loan, M., Richmond, W.R. and Parkinson, G.M. (2005), *J. Cryst. Growth.,* Vol. 275, pp. 1875-1881.
32. Olowe, A.A., Génin, J.-M.R. and Bauer, Ph. (1989), *Hyperfine Interact.,* Vol. 46, pp. 437-443.
33. Perales, O. and Umetsu, Y. (2000), *Hydrometallurgy*, Vol. 55, pp. 35-56.
34. Peulon, S., Legrand, L., Antonyand, H. and Chaussé, A. (2003), *Electrochem. Commun.*, Vol. 5, pp. 208-213.
35. Refait, Ph., Bernali, O., Abdelmoula, M. and Geninand, J.-M.R. (2003), *Corros. Sci.,* Vol. 45, pp. 2435-2449.
36. Refait, P., Memet, J.-B., Bon, C., Sabota, R. and Génin, J.-M.R. (2003), *Corros. Sci.,* Vol. 45 No 4, pp. 833-845.
37. Ruby, C., Gehin, A., Aissa, R. and Genin, J.-M.R. (2006), *Corros. Sci.,* Vol. 48, pp. 3824-3837.
38. Russell, M.J., Hall, A.J., Boyce, A.J. and Fallick, A.E. (2005), *Bull. Soc. Econ. Geol.*, Vol. 100 No 3, pp. 419-438.
39. Schwertmann, U. and Carlson, L. (2005), *Clay Miner.,* Vol. 40, pp. 63-66.
40. Schwertmann, U. and Cornell, R.M. (2000), *Iron oxides in the laboratory: preparation and haracterization,* Weinheim, New York, Bazel, Cambridge, 188 p.
41. Schwertmann, U. and Fechter, H. (1994), *Clay Miner.*, Vol. 29, pp. 87-92.
42. Tamaura, Y., Yoshida, T. and Katsura, T. (1984), *Bull. Chem. Soc. Jap.,* Vol. 57, pp. 2411-2416.
43. Washeda, Y. and Suzuki, S. (2005), *Characterization of Corrosion products on Steel Surface*, Springer, 297 p.
44. Yu, J.-Y., Heo, B., Choi, I.-K., Cho, J.-P. and Chang, H.-W. (1999), *Geochim. et cosmochim. acta*, Vol. 63, pp. 3407-3416.
45. Yu, J.-Y., Park, M. and Kim, J. (2002), *Geochem. Journ.*, Vol. 36 No 2, pp. 119-132.

О.М. Лавриненко, Ю.С. Щукін

Інститут біоколоїдної хімії ім. Ф.Д. Овчаренка НАН України
03680, м. Київ-142, Україна, бульв. Акад. Вернадського, 42
E-mail: alena-lavry@yandex.ru

РОЗВИТОК ГІДРОКСИСУЛЬФАТНОГО *GREEN RUST* НА ПОВЕРХНІ СТАЛІ,
ЯКА КОНТАКТУЄ З ВОДНИМИ РОЗЧИНАМИ FeSO$_4$ І Fe$_2$(SO$_4$)$_3$

За допомогою методів рентгенофазового анализу *in situ* та сканувальної електронної мікроскопії проведено дослідження процесів формування та перетворення гідроксисульфатного *Green Rust GR*(SO$_4$$^{2-}$) (сульфатного фойгериту) на поверхні сталі, яка контактує з водними розчинами FeSO$_4$ та Fe$_2$(SO$_4$)$_3$ за окисних та відновних умов. Показано, що колоїдно-хімічний механізм розвитку мінеральних фаз визначається локальними фізико-хімічними умовами на поверхні сталі. Так, на її анодних ділянках відбувається розчинення та переосадження слабкоокристалізованих мінералів в ряду: швертманніт → гетит (феригідрит) → *Green Rust*, а на катодних ділянках — твердо-

фазне перетворення *Green Rust* в його окиснену форму Fe(III)−GR або лепідокроіт. Формування нанорозмірних частинок магнетиту реалізується за обмеженого надходження кисню та обумовлено взаємодією міцелярних структур Fe(II) і Fe(III) або продуктів розчинення *Green Rust*.

Ключові слова: Fe(II)−Fe(III) шаруваті подвійні гідроксиди, гідроксисульфатний *Green Rust*, наночастинки, сульфатний фойгерит, швертманніт, Fe(III)−*Green Rust*, лепідокроіт, магнетит, поверхня сталі, окисно-відновні умови.

Е.Н. Лавриненко, Ю.С. Щукин

Институт биоколлоидной химии им. Ф.Д. Овчаренко НАН Украины
03680, г. Киев-142, Украина, бульв. Акад. Вернадского, 42
E-mail: alena-lavry@yandex.ru

РАЗВИТИЕ ГИДРОКСИСУЛЬФАТНОГО *GREEN RUST* НА ПОВЕРХНОСТИ СТАЛИ, КОНТАКТИРУЮЩЕЙ С ВОДНЫМИ РАСТВОРАМИ $FeSO_4$ И $Fe_2(SO_4)_3$

С помощью методов рентгенофазового анализа *in situ* и сканирующей электронной микроскопии проведено исследование процессов формирования и трансформации гидроксисульфатного *Green Rust* $GR(SO_4^{2-})$ (сульфатного фойгерита) на поверхности стали, контактирующей с водными растворами $FeSO_4$ и $Fe_2(SO_4)_3$ в окислительных и восстановительных условиях. Показано, что коллоидно-химический механизм развития минеральных фаз определяется локальными физико-химическими условиями на поверхности стали. Так, на ее анодных участках происходит растворение и переосаждение слабоокристаллизованных дисперсных минералов в ряду: швертманнит → гетит (ферригидрит) → *Green Rust*, а на катодных участках — твердофазная трансформация *Green Rust* в его окисленную форму Fe(III)−GR или лепидокрокит. Образование наноразмерных частиц магнетита проходит в условиях ограниченного доступа кислорода и обусловлено взаимодействием мицеллярных структур Fe(II) и Fe(III) или продуктов растворения *Green Rust*.

Ключевые слова: Fe(II)−Fe(III) слоистые двойные гидроксиды, гидроксисульфатный *Green Rust*, наночастицы, сульфатный фойгерит, швертманнит, Fe(III)−*Green Rust*, лепидокрокит, магнетит, поверхность стали, окислительно-восстановительные условия.